Acta Crystallographica Section B
**Structural Science**
ISSN 0108-7681

# Structural behaviour of synthetic $Co_2SiO_4$ at low temperatures

**Andrew Sazonov,[a,b]* Martin Meven,[b] Vladimir Hutanu,[a,b] Volker Kaiser,[a] Gernot Heger,[a] Dmytro Trots[c] and Michael Merz[a,d]**

[a]Institut für Kristallographie, Rheinisch-Westfälische Technische Hochschule (RWTH) Aachen, D-52066 Aachen, Germany, [b]Forschungsneutronenquelle Heinz Maier-Leibnitz (FRM II), Technische Universität München, D-85747 Garching, Germany, [c]Hamburger Synchrotronstrahlungslabor (HASYLAB), Deutsches Elektronen-Synchrotron (DESY), D-22607 Hamburg, Germany, and [d]Forschungszentrum Karlsruhe, Institut für Festkörperphysik, D-76021 Karlsruhe, Germany

Correspondence e-mail: andrew.sazonov@frm2.tum.de

Received 12 June 2008
Accepted 6 October 2008

Synthetic $Co_2SiO_4$ has an olivine structure with isolated $SiO_4$ groups (space group *Pnma*) and shows magnetic ordering below 50 K. Single-crystal neutron diffraction was applied to determine precise crystal structure parameters at low temperatures. No structural phase transition was revealed in the temperature range 2.5–300 K. Lattice parameters were determined by high-resolution X-ray powder diffraction between 15 and 300 K. There is a clear evidence of an anomalous thermal expansion related to the magnetic phase transition which can be attributed to magnetostriction.

## 1. Introduction

Compounds of the chemical formula $M_2SiO_4$ with olivine-type structure are of fundamental importance for geologists and mineralogists because of the presence of a huge amount of the olivines in the earth's upper mantle. Here, $M$ is mainly Fe, Mg and Mn with small amounts of Ni, Ca, Co and Zn in mixed crystals.

The crystal structure of Mg/Fe olivine was determined long ago (Bragg & Brown, 1926). Since then, olivines have also been of great interest to crystallographers, especially because of the peculiarities of their magnetic structure. The magnetic properties of $M_2SiO_4$ depend strongly on the type of $M^{2+}$ cation.

Many studies provided abundant data on the olivine-type oxides, especially at or above room temperature and at high pressure. However, there is still a lack of information on the magnetic properties and the thermal evolution of the crystal structure below room temperature for some olivines. One of the less-studied olivine-type silicates is the synthetic cobalt olivine, $Co_2SiO_4$. To our knowledge, the structural parameters of $Co_2SiO_4$ were published only from X-ray diffraction analyses at room temperature and above. However, neutrons are the most appropriate probe for studies of both crystal and magnetic structures. Firstly, as the neutron interacts with nuclei, there is no fall-off in the scattering cross-section with increasing scattering angle. This enables us to determine the atomic distribution more precisely than in the case of X-rays. Secondly, the fact that the neutron cross-sections do not depend on the atomic numbers means that light atoms (the O atoms in this case) can be localized as easily as heavy ones. Finally, the magnetic moment of neutrons allows the magnetic structures to be determined.

Structure analyses of $Co_2SiO_4$ single crystals and powder samples were already performed at room temperature (Ghose & Wan, 1974; Miyake *et al.*, 1987; Morimoto *et al.*, 1974; Tamada *et al.*, 1983) and the magnetic structure was studied below 50 K (Lottermoser & Fuess, 1988; Ballet *et al.*, 1989). However, details of the crystal structure below room

**Table 1**
Single-crystal neutron diffraction experimental and refinement details.

| | 300 K | 55 K | 2.5 K |
|---|---|---|---|
| Crystal data | | | |
| Chemical formula | $Co_2SiO_4$ | $Co_2SiO_4$ | $Co_2SiO_4$ |
| $M_r$ | 209.95 | 209.95 | 209.95 |
| Cell setting, space group | Orthorhombic, *Pnma* | Orthorhombic, *Pnma* | Orthorhombic, *Pnma* |
| Temperature (K) | 300 | 55 | 2.5 |
| $a, b, c$ (Å) | 10.3005 (1), 6.0028 (1), 4.7816 (1) | 10.2869 (1), 5.9889 (1), 4.7781 (1) | 10.2864 (1), 5.9872 (1), 4.7785 (1) |
| $V$ (Å$^3$) | 295.66 | 294.37 | 294.29 |
| $Z$ | 4 | 4 | 4 |
| $D_x$ (Mg m$^{-3}$) | 4.715 | 4.715 | 4.715 |
| Radiation type | Constant wavelength neutron diffraction radiation | Constant wavelength neutron diffraction radiation | Constant wavelength neutron diffraction radiation |
| $\mu$ (mm$^{-1}$) | 0.03 | 0.03 | 0.03 |
| Crystal form, colour | Parallelepiped, dark violet | Parallelepiped, dark violet | Parallelepiped, dark violet |
| Crystal size (mm) | 3 × 2 × 2 | 3 × 2 × 2 | 3 × 2 × 2 |
| Data collection | | | |
| Diffractometer | Single-crystal HEiDi | Single-crystal HEiDi | Single-crystal HEiDi |
| Data collection method | $\omega$ scans | $\omega$ scans | $\omega$ scans |
| Absorption correction | Numerical | Numerical | Numerical |
| $T_{min}$ | 0.918 | 0.915 | 0.915 |
| $T_{max}$ | 0.946 | 0.947 | 0.947 |
| No. of measured, independent and observed reflections | 2920, 1624, 1341 | 2118, 1465, 1098 | 3226, 1424, 1070 |
| Criterion for observed reflections | $I>2\sigma(I)$ | $I>2\sigma(I)$ | $I>2\sigma(I)$ |
| $R_{int}$ | 0.034 | 0.028 | 0.033 |
| $\theta_{max}$ (°) | 37.4 | 37.9 | 37.9 |
| No. and frequency of standard reflections | 3 every 360 min | 3 every 360 min | 3 every 360 min |
| Intensity decay (%) | 0.7 | 0.7 | 0.7 |
| Refinement | | | |
| Refinement on | $F^2$ | $F^2$ | $F^2$ |
| $R[F^2>2\sigma(F^2)]$, $wR(F^2)$, $S$ | 0.034, 0.054, 1.28 | 0.029, 0.035, 1.10 | 0.033, 0.044, 1.49 |
| No. of reflections | 1341 | 1098 | 1070 |
| No. of parameters | 46 | 46 | 50 |
| Weighting scheme | $w = 1/\sigma^2(F_o^2)$ | $w = 1/\sigma^2(F_o^2)$ | $w = 1/\sigma^2(F_o^2)$ |
| $(\Delta/\sigma)_{max}$ | < 0.0001 | < 0.0001 | < 0.0001 |
| $\Delta\rho_{max}$, $\Delta\rho_{min}$ (e Å$^{-3}$) | 0.19, −0.16 | 0.17, −0.13 | 0.11, −0.12 |
| Extinction method | Anisotropic | Anisotropic | Anisotropic |
| Extinction coefficient | 0.10 (1), 0.28 (1), 1.23 (4), 0.04 (1), −0.06 (3), −0.04 (6) | 0.11 (1), 0.07 (4), 1.27 (4), 0.18 (3), 0.27 (2), 0.03 (4) | 0.16 (1), 0.35 (4), 1.43 (3), 0.00 (3), 0.27 (2), 0.22 (4) |

temperature were not published. Moreover, the magnetic behaviour of $Co_2SiO_4$ has not been fully understood up until now, especially concerning the effects of covalency, superexchange coupling and frustration.

In order to clarify the magnetic interactions in this compound, polarized neutron diffraction measurements are necessary.

The main goal of the present study is to determine precisely the changes in the crystal structure of $Co_2SiO_4$ in the temperature range 2.5–300 K by means of powder X-ray and single-crystal neutron diffraction measurements. The room-temperature results are compared with those from previously reported X-ray diffraction experiments (Ghose & Wan, 1974; Miyake *et al.*, 1987; Morimoto *et al.*, 1974; Tamada *et al.*, 1983). The high accuracy in the determination of the lattice parameters, the atomic positions and the atomic displacement parameters (ADPs) in this study was essential to correctly interpret the experimental electron and spin-density maps obtained in our experiments with synchrotron radiation and polarized neutrons on single crystals (will be published elsewhere). Thus, these investigations are part of our program aimed at the understanding of the peculiarities of the crystal structure and magnetic properties of cobalt olivine in detail.

## 2. Experimental

### 2.1. Sample preparation

CoO and $SiO_2$ powders were weighed in stoichiometric proportions and mixed. The mixture was placed in an $Al_2O_3$ crucible and heated in a furnace at 1400 K for 48 h in air. The procedure was repeated and then the powder was re-ground and pressed hydrostatically under a pressure of 55 MPa cm$^{-2}$ in a plastic cylindrical balloon. Thus, a rod of $\sim$ 7 mm in diameter and 80 mm in length was prepared and finally sintered at the same conditions as described above. The parts of this rod were then used as the feed and seed rods during the crystal growth procedure. Crystal growth was performed by the floating-zone method using a mirror furnace (Crystal System Inc., Model No. FZT-10000-H-II-VP). The furnace is

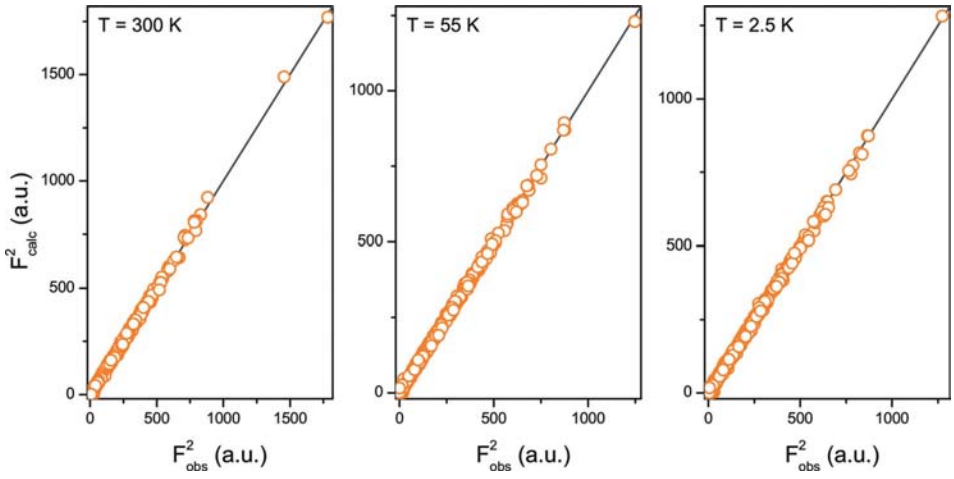


**Figure 1**
Results of the refinement for $Co_2SiO_4$ from our single-crystal neutron diffraction data at different temperatures. The experimental $F^2$ values ($F^2_{obs}$) are plotted against the calculated ones ($F^2_{calc}$).

equipped with four IR halogen lamps as the heat source of a maximum power of 1 kW each. Feed and seed rods were rotated in the furnace in opposite directions with a rotation speed of $\sim 30$ r.p.m. The growth rate was $\sim 1.5$ mm $h^{-1}$. The length of the molten zone was $\sim 5$ mm and the power required to maintain this length value was $\sim 2$ kW. Thus, a large dark purple single crystal with a dimension of about 6 mm in diameter and 15 mm in length was obtained after several cycles of the growth process.

### 2.2. Single-crystal neutron diffraction

To study structural parameters such as the atomic positions and ADPs in detail, especially those of the O atoms, a small $Co_2SiO_4$ single crystal of $3 \times 2 \times 2$ mm was cut from the large as-grown crystal. This sample was studied at the neutron source Heinz Maier-Leibnitz (FRM II) on the hot four-circle diffractometer HEiDi (Meven *et al.*, 2007). Using a Cu-(420) monochromator a short wavelength of 0.552 (1) Å was obtained with a high flux density of $>2 \times 10^6$ neutrons $s^{-1}$ $cm^{-2}$. The large available $q$ space ($\sin\theta/\lambda$ range) at this wavelength yields a large number of symmetrically nonequivalent measurable Bragg reflections. Thus, not only the positional parameter but also other parameters such as the ADPs can be refined with very small error bars $<10^{-4}$. Additionally, typical sources of systematical errors such as the extinction effect are significantly dampened at this wavelength. For low-temperature experiments a He closed-cycle cryostat was mounted in the Eulerian cradle of the diffractometer. The sample crystal was wrapped in Al foil in order to ensure homogeneity of the temperature. The temperature was measured and controlled by a diode sensor near the sample position and a stability of $\pm 0.1$ K was achieved. The absolute temperatures of the measurements were obtained by using an additional temperature sensor at the sample position. The corrected integrated intensities of the measured reflections were obtained using the program *PRON*2K.[1] Numerical absorption correction was performed with the program *TBAR*.[2] The atomic positions and displacement parameters of $Co_2SiO_4$ were refined using the single-crystal option of the *FULLPROF* program (Rodríguez-Carvajal, 1993). Standard single-crystal refinement programs like *SHELX* or *JANA*2000 are not appropriate for the low-temperature data because of the additional magnetic contributions to the Bragg intensities below 50 K. Experimental and refinement details for single-crystal neutron diffraction at 2.5, 55 and 300 K are summarized in Table 1.[3]

### 2.3. X-ray powder diffraction

In order to determine the lattice parameters of $Co_2SiO_4$, powder samples were finely ground from a part of the as-grown single crystal and studied by means of conventional (laboratory) X-ray powder diffraction using the X'Pert PRO instrument (PANalytical) at the Institute of Crystallography, RWTH Aachen. The data were collected in Bragg–Brentano geometry with Cu $K\alpha_{1,2}$ radiation. Owing to the $\theta$–$\theta$ geometry of the diffractometer, the flat sample stayed fixed in the horizontal plane. The intensity was recorded by a position-sensitive detector (X'Celerator, PANalytical). The sample holder consisted of a copper plate mounted on top of a double-stage He closed-cycle refrigerator. The temperature of the sample was controlled by two diode sensors and a stability of $\pm 0.1$ K was achieved. One sensor was in direct contact with the sample holder, the other one was situated close to the heater at the cold-head itself. Diffraction patterns were measured at various temperatures between 19 and 300 K in the $2\theta$ range from 10 to 120°. Silicon was used as an internal standard to ensure a high accuracy for the determination of the lattice parameters and to compensate for the temperature-dependent displacement errors. Lattice parameters of $Co_2SiO_4$ were obtained by whole pattern fitting using the LeBail method implemented in the *FULLPROF* program (Rodríguez-Carvajal, 1993).

[1] Program for data reduction of *DIF*4. Version of Institut für Kristallographie, RWTH Aachen.
[2] Program for calculating absorption, mean paths and extinction for single crystals (Paul Scherrer Institut).
[3] Supplementary data for this paper are available from the IUCr electronic archives (Reference: BP5014). Services for accessing these data are described at the back of the journal.

In order to prove the results of our laboratory X-ray powder diffraction study, which revealed an unusual behaviour of the lattice parameters at low temperature, high-resolution experiments were carried out at the synchrotron facility HASYLAB/DESY with the powder diffractometer at beamline B2 (Knapp, Baehtz *et al.*, 2004). The powder sample consisted of a completely filled and sealed quartz capillary of 0.3 × 30 mm. It was mounted with a capillary spinner in Debye–Scherrer geometry inside a He closed-cycle cryostat (Ihringer & Küster, 1993) equipped with a silicon diode as the temperature sensor. A wavelength of 0.50206 (1) Å was selected from the direct white synchrotron beam using a Si(111) double flat-crystal monochromator and determined from eight reflection positions of a $LaB_6$ reference sample (NIST SRM 660a). The beam size of 0.4 × 3 mm at the sample position was cut by slits. All diffraction patterns were collected using an on-site readable position-sensitive image-plate detector ($2\theta$ range 4–55°; Knapp, Joco *et al.*, 2004). Several patterns were collected during the cooling process at a continuous temperature decrease down to 15 K with time intervals of approximately 10 min per pattern, whereas the data collection at fixed temperatures was applied during the heating from 15 up to 300 K (on average approximately 30 min per pattern). Structure parameters of $Co_2SiO_4$ were obtained from Rietveld refinements using the *FULLPROF* program (Rodríguez-Carvajal, 1993). Experimental details for powder neutron diffraction at selected temperatures are summarized in Table 2.

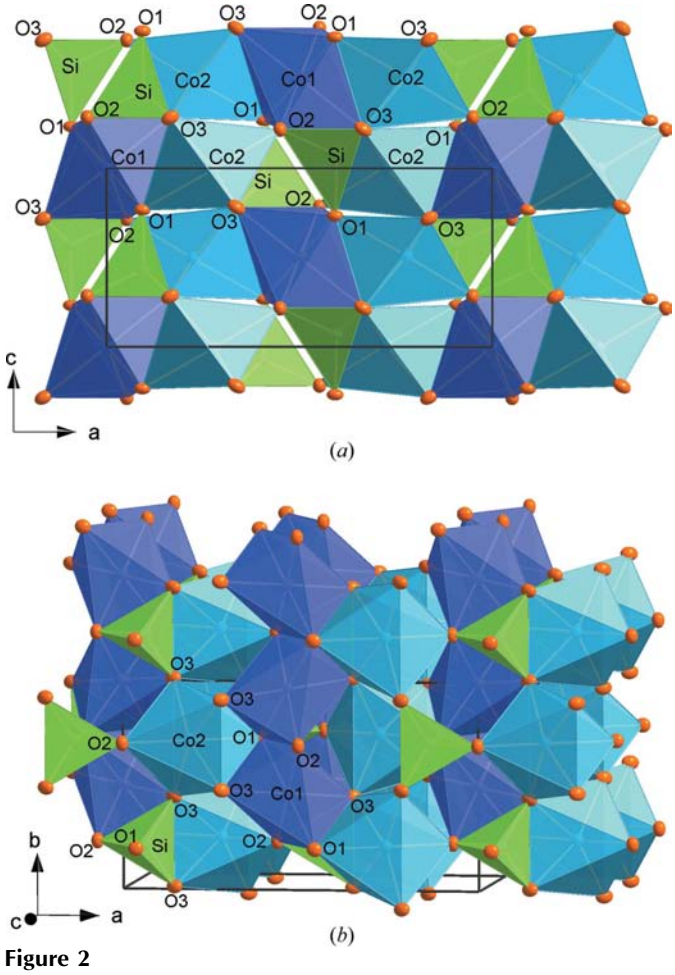


**Figure 2**
Structure of $Co_2SiO_4$ olivine at room temperature. (*a*) Projection onto the *ac* plane; (*b*) clinographic view. Displacement ellipsoids are plotted at the 95% probability level. This and the following molecular graphics were drawn with *DIAMOND* (Brandenburg, 1999).

## 3. Results and discussion

### 3.1. Structure of $Co_2SiO_4$ at room temperature

In order to prove the quality of our $Co_2SiO_4$ single crystal and to compare its structural parameters with those reported in the literature by Ghose & Wan (1974), Miyake *et al.* (1987), Morimoto *et al.* (1974) and Tamada *et al.* (1983), we performed a neutron diffraction study at room temperature on the single-crystal diffractometer HEiDi at FRM II. The observed reflection profiles correspond to the instrumental resolution. This demonstrates the good quality of the crystal. Bragg reflection intensities were collected up to $\sin\theta/\lambda \simeq 1.04$ Å$^{-1}$ [$\lambda$ = 0.552 (1) Å]. The stability of the experiment was controlled by the repeated measurement of standard reflections. There were 2920 Bragg reflections measured and averaged over symmetry equivalents to yield a total of 1624 independent reflections with an internal $R$ value of $R_{int}$ = 0.034. Then, reflections with $I \leq 2\sigma(I)$ were deleted, and the remaining 1341 reflections were used for the structure refinement. Lattice parameters were taken from the synchrotron powder diffraction data (see below). Other starting parameters for the least-squares refinements were obtained from Tamada *et al.* (1983). Positional parameters and anisotropic ADPs were refined in combination with an overall scale factor. Extinction effects were corrected according to an anisotropic model, as implemented in the *FULLPROF* program (Rodríguez-Carvajal, 1993). The results of the refinements are shown in Fig. 1 and Table 1.

The structure of $Co_2SiO_4$ can be characterized by a hexagonal closed packing of O atoms. It crystallizes in the orthorhombic *Pnma* space group with four formula units in the unit cell ($Z = 4$; Fig. 2). There are two crystallographically

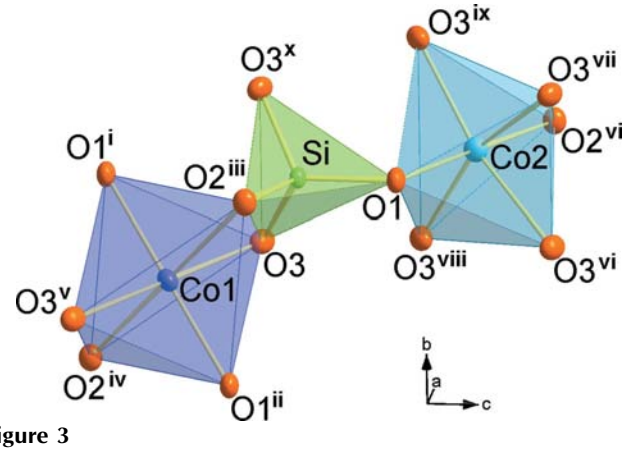


**Figure 3**
Clinographic view of the $CoO_6$ and $SiO_4$ polyhedra in $Co_2SiO_4$ at room temperature. Displacement ellipsoids are plotted at the 95% probability level. See Table 3 for the symmetry codes.

**Table 2**
Synchrotron powder diffraction experimental and refinement details.

| | 180 K | 100 K | 50 K | 35 K | 15 K |
|---|---|---|---|---|---|
| Crystal data | | | | | |
| Chemical formula | $Co_2SiO_4$ | $Co_2SiO_4$ | $Co_2SiO_4$ | $Co_2SiO_4$ | $Co_2SiO_4$ |
| $M_r$ | 209.95 | 209.95 | 209.95 | 209.95 | 209.95 |
| Cell setting, space group | Orthorhombic, *Pnma* | Orthorhombic, *Pnma* | Orthorhombic, *Pnma* | Orthorhombic, *Pnma* | Orthorhombic, *Pnma* |
| *a*, *b*, *c* (Å) | 10.2928 (1), 5.9927 (1), 4.7795 (1) | 10.2891 (1), 5.9899 (1), 4.7785 (1) | 10.2868 (1), 5.9888 (1), 4.7780 (1) | 10.2873 (1), 5.9879 (1), 4.7789 (1) | 10.2876 (1), 5.9877 (1), 4.7789 (1) |
| $V$ (Å$^3$) | 294.804 (6) | 294.499 (6) | 294.348 (6) | 294.374 (6) | 294.373 (6) |
| $Z$ | 4 | 4 | 4 | 4 | 4 |
| Radiation type | Synchrotron | Synchrotron | Synchrotron | Synchrotron | Synchrotron |
| Wavelength (Å) | 0.50206 (1) | 0.50206 (1) | 0.50206 (1) | 0.50206 (1) | 0.50206 (1) |
| Specimen form, colour | Powder, violet | Powder, violet | Powder, violet | Powder, violet | Powder, violet |
| Specimen size (mm) | 0.3 × 30 | 0.3 × 30 | 0.3 × 30 | 0.3 × 30 | 0.3 × 30 |
| Data collection | | | | | |
| Data collection method | $2\theta$ scans | $2\theta$ scans | $2\theta$ scans | $2\theta$ scans | $2\theta$ scans |
| $2\theta$ range (°) | 4–55 | 4–55 | 4–55 | 4–55 | 4–55 |
| $2\theta$ step size (°) | 0.004 | 0.004 | 0.004 | 0.004 | 0.004 |
| Refinement | | | | | |
| Refinement method | Rietveld | Rietveld | Rietveld | Rietveld | Rietveld |
| $R_p$, $R_{wp}$ | 0.039, 0.050 | 0.041, 0.052 | 0.041, 0.052 | 0.040, 0.050 | 0.042, 0.054 |
| $R_{Bragg}$, $S$ | 0.034, 3.21 | 0.037, 3.27 | 0.036, 3.19 | 0.035, 3.15 | 0.037, 3.22 |
| Excluded region(s) | None | None | None | None | None |
| Profile function | Pseudo-Voigt | Pseudo-Voigt | Pseudo-Voigt | Pseudo-Voigt | Pseudo-Voigt |
| No. of parameters | 33 | 33 | 33 | 33 | 33 |
| No. of data points | 12 751 | 12 751 | 12 751 | 12 751 | 12 751 |

nonequivalent $Co^{2+}$ sites, namely Co1(4*a*) with inversion symmetry $\bar{1}$ and Co2(4*c*) with mirror symmetry *m* (Figs. 2 and 3). The Co1 cation is coordinated by six O atoms with Co—O distances ranging between 2.0929 (2) and 2.1715 (2) Å at room temperature with an average Co1—O distance of 2.1200 Å. The $Co1O_6$ octahedra are interconnected by common edges and form single chains parallel to *b* (Fig. 2). Besides the two $Co1O_6$ neighbour octahedra there are four $Co2O_6$ octahedra attached to each $Co1O_6$ by common corners and two $Co2O_6$ by common edges. The Co2 cations also form octahedra with Co—O distances within 2.0684 (4) and 2.2250 (6) Å with an average Co2—O distance of 2.1402 Å at room temperature. The $Co2O_6$ octahedra are attached on alternate sides to the $Co1O_6$ chains in a way that the whole arrangement of $Co1O_6$ and $Co2O_6$ octahedra forms zigzag chains along the *b* direction. Each $Co2O_6$ octahedron has four $Co2O_6$ neighbours with common corners. On the other hand, there are four $Co1O_6$ neighbour octahedra connected to $Co2O_6$ by common corners and two by common edges. The Si cations are coordinated by four O atoms forming the $SiO_4$ tetrahedra which are not linked (Figs. 2 and 3).

Our refined positional parameters at room temperature are in very good agreement [$<2\sigma(I)$] with data from the literature by Ghose & Wan (1974), Miyake *et al.* (1987), Morimoto *et al.* (1974) and Tamada *et al.* (1983). For instance, a comparison of the Co—O distances at room temperature is shown in Fig. 4. The detailed structural parameters of $Co_2SiO_4$ at 300 K are deposited in the CIF. Selected interatomic distances and angles in $Co_2SiO_4$ are summarized in Table 3.

It is worth noting that Bragg intensities contain information on the electron-density distribution (X-ray diffraction) or the nuclear densities (neutron diffraction) smeared by dynamic and static displacements. In many combined X-ray and neutron diffraction studies it has been shown that for non-H atoms satisfactory correspondence between the positional parameters determined by these two techniques can be achieved, see for instance our example in Fig. 4. On the contrary, the agreement between the ADPs determined in parallel X-ray and neutron experiments is very often less satisfying because of numerous systematic errors. For precise work, even in the case of neutrons, measurement of many

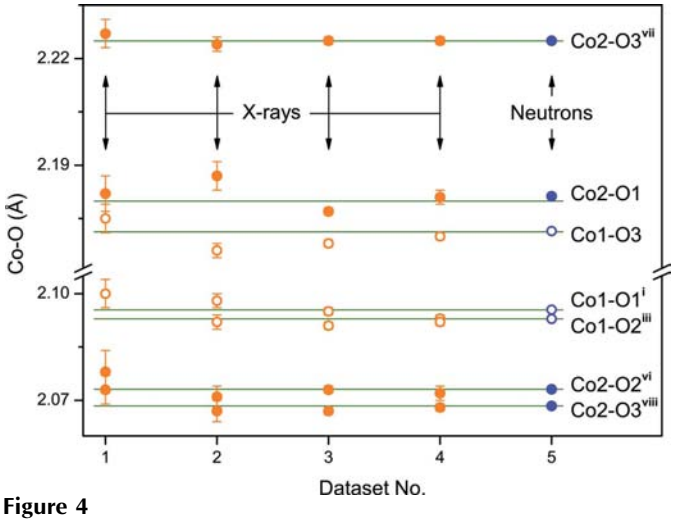


**Figure 4**
Comparison of the Co—O distances from different measurements at room temperature. Dataset No. 1 corresponds to Morimoto *et al.* (1974), 2 – Ghose & Wan (1974), 3 – Tamada *et al.* (1983), 4 – Miyake *et al.* (1987), 5 – our single-crystal neutron diffraction data (error bars from the refinement are smaller than the symbols). Solid lines represent weighted averaged values calculated for all measurements. See Table 3 for the symmetry codes.

equivalent reflections with a crystal of good quality is necessary. See for instance the $\sin\theta/\lambda$ dependency of the displacement parameters in Fig. 5 determined from our single-crystal neutron diffraction measurements at room temperature.

The lattice parameters at room temperature were obtained from X-ray powder diffraction measurements (Fig. 6). They are also in close agreement with the literature data (Ghose & Wan, 1974; Matsui & Syono, 1968; Miyake *et al.*, 1987; Morimoto *et al.*, 1974; Müller-Sommer *et al.*, 1997; Nomura *et al.*, 1964; Tamada *et al.*, 1983).

### 3.2. Structural variations with temperature

**3.2.1. Lattice parameters**. Fig. 6 shows the variation of the lattice parameters and the unit-cell volume of $Co_2SiO_4$ with temperature over the complete temperature range covered in our X-ray powder diffraction experiments. The Rietveld fit of the synchrotron powder diffraction data at 35 K is shown in Fig. 7 as an example. Refinement results for selected temperatures are summarized in Table 2. The lattice parameters of $Co_2SiO_4$ exhibit an anomaly at *ca* 50 K (Fig. 6). Neither splitting of reflections due to symmetry changes nor broadening were observed in the powder diffraction patterns in the temperature range from 300 down to 15 K; the patterns were successfully indexed according to the space group *Pnma*. Furthermore, our single-crystal neutron data did not show any reflections violating the *Pnma* symmetry. Thus, we conclude that the *Pnma* symmetry is retained below room temperature. The anomaly in the anisotropic thermal expansion can therefore be associated with the magnetic phase transition taking place at 50 K (Lottermoser & Fuess, 1988; Ballet *et al.*, 1989). All lattice parameters show variations at this temperature which can be related to magnetostriction effects. The unit-cell volume is almost unaffected. An abrupt elongation and contraction below approximately 50 K were observed along the *c* and *b* axes, respectively, whereas the lattice parameter *a* keeps constant in the range between 15 and 50 K (see Fig. 6). Note that both the laboratory and synchrotron X-ray powder diffraction data are in excellent agreement, without any adjustment.

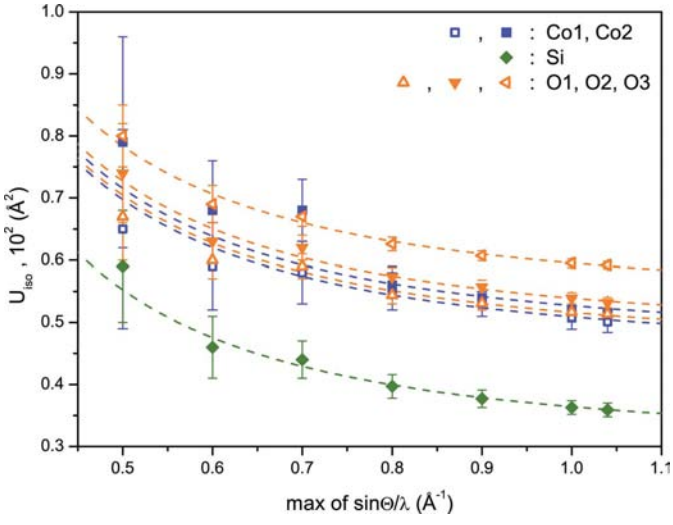


**Figure 5**
An example of the accuracy of the refined isotropic ADPs for $Co_2SiO_4$ as a function of the measured $\sin\theta/\lambda$ range from our single-crystal neutron diffraction data at room temperature. The fits are used as guides to the eye.

**Table 3**
Interatomic distances (Å) and angles (°) in $Co_2SiO_4$ from single-crystal neutron diffraction at different temperatures.

| | 300 K | 55 K | 2.5 K |
|---|---|---|---|
| Co1 octahedron | | | |
| Co1—O1$^{i}$, Co1—O1$^{ii}$ | 2.0955 (2) | 2.0907 (2) | 2.0901 (2) |
| Co1—O2$^{iii}$, Co1—O2$^{iv}$ | 2.0929 (2) | 2.0896 (2) | 2.0885 (2) |
| Co1—O3, Co1—O3$^{v}$ | 2.1715 (2) | 2.1678 (1) | 2.1691 (2) |
| ⟨Co1—O⟩ | 2.1200 | 2.1160 | 2.1159 |
| O1$^{i}$—Co1—O1$^{ii}$ | 180.00 | 180.00 | 180.00 |
| O1$^{i}$—Co1—O2$^{iii}$, O1$^{ii}$—Co1—O2$^{iv}$ | 86.90 (2) | 86.96 (2) | 86.96 (2) |
| O1$^{i}$—Co1—O2$^{iv}$, O1$^{ii}$—Co1—O2$^{iii}$ | 93.10 (1) | 93.04 (1) | 93.05 (1) |
| O1$^{i}$—Co1—O3, O1$^{ii}$—Co1—O3$^{v}$ | 84.87 (1) | 84.92 (1) | 84.95 (1) |
| O1$^{i}$—Co1—O3$^{v}$, O1$^{ii}$—Co1—O3 | 95.13 (2) | 95.10 (1) | 95.05 (2) |
| O2$^{iii}$—Co1—O2$^{iv}$ | 180.00 | 180.00 | 180.00 |
| O2$^{iii}$—Co1—O3, O2$^{iv}$—Co1—O3$^{v}$ | 74.15 (1) | 74.29 (1) | 74.30 (1) |
| O2$^{iii}$—Co1—O3$^{v}$, O2$^{iv}$—Co1—O3 | 105.85 (2) | 105.72 (1) | 105.70 (2) |
| O3—Co1—O3 | 180.00 | 180.00 | 180.00 |
| Co2 octahedron | | | |
| Co2—O1 | 2.1813 (8) | 2.1759 (6) | 2.1756 (7) |
| Co2—O2$^{vi}$ | 2.0731 (8) | 2.0731 (6) | 2.0751 (6) |
| Co2—O3$^{vii}$, Co2—O3$^{vi}$ | 2.2250 (6) | 2.2193 (5) | 2.2194 (5) |
| Co2—O3$^{viii}$, Co2—O3$^{ix}$ | 2.0684 (4) | 2.0647 (4) | 2.0629 (4) |
| ⟨Co2—O⟩ | 2.1402 | 2.1361 | 2.1359 |
| O1—Co2—O2$^{vi}$ | 178.32 (4) | 178.30 (3) | 178.26 (3) |
| O1—Co2—O3$^{vii}$, O1—Co2—O3$^{vi}$ | 81.62 (3) | 81.71 (2) | 81.76 (2) |
| O1—Co2—O3$^{viii}$, O1—Co2—O3$^{ix}$ | 91.09 (3) | 91.13 (2) | 91.15 (2) |
| O2$^{vi}$—Co2—O3$^{vii}$, O2$^{vi}$—Co2—O3$^{vi}$ | 97.02 (3) | 96.92 (2) | 96.83 (2) |
| O2$^{vi}$—Co2—O3$^{viii}$, O2$^{vi}$—Co2—O3$^{ix}$ | 89.87 (3) | 89.84 (2) | 89.85 (2) |
| O3$^{viii}$—Co2—O3$^{vi}$, O3$^{ix}$—Co2—O3$^{vii}$ | 88.60 (2) | 88.69 (2) | 88.67 (2) |
| O3$^{viii}$—Co2—O3$^{vii}$, O3$^{ix}$—Co2—O3$^{vi}$ | 159.48 (2) | 159.75 (2) | 159.76 (2) |
| O3$^{vii}$—Co2—O3$^{vi}$ | 71.43 (2) | 71.60 (2) | 71.63 (2) |
| O3$^{viii}$—Co2—O3$^{ix}$ | 110.80 (2) | 110.49 (2) | 110.52 (2) |
| Si tetrahedron | | | |
| Si—O1 | 1.6208 (5) | 1.6207 (4) | 1.6199 (4) |
| Si—O2$^{iii}$ | 1.6554 (5) | 1.6555 (4) | 1.6551 (5) |
| Si—O3, Si—O2$^{x}$ | 1.6392 (3) | 1.6397 (3) | 1.6409 (3) |
| ⟨Si—O3⟩ | 1.6387 | 1.6389 | 1.6392 |
| O1—Si—O2$^{iii}$ | 113.50 (3) | 113.47 (3) | 113.56 (3) |
| O1—Si—O3, O1—Si—O3$^{x}$ | 115.80 (3) | 115.90 (2) | 115.88 (2) |
| O2$^{iii}$—Si—O3, O2$^{iii}$—Si—O3$^{x}$ | 102.62 (3) | 102.58 (2) | 102.59 (2) |
| O3—Si—O3$^{x}$ | 104.81 (2) | 104.69 (2) | 104.62 (2) |

Symmetry codes: (i) $x, y, z-1$; (ii) $-x, y-\frac{1}{2}, -z+1$; (iii) $x-\frac{1}{2}, -y+\frac{1}{2}, -z+\frac{1}{2}$; (iv) $-x+\frac{1}{2}, -y, z-\frac{1}{2}$; (v) $-x, -y, -z$; (vi) $x, y, z+1$; (vii) $x, -y+\frac{1}{2}, z+1$; (viii) $-x+\frac{1}{2}, -y, z+\frac{1}{2}$; (ix) $-x+\frac{1}{2}, y+\frac{1}{2}, z+\frac{1}{2}$; (x) $x, -y+\frac{1}{2}, z$.

The solid curves in Fig. 6 represent a fit of the experimental lattice parameters to a sigmoidal function (Boltzmann model) in the temperature range from 51 to 300 K. The fitting curve was also extended below 51 K in order to show the deviation from the high-temperature ($T$>50 K) predicted normal behaviour at low-temperature ($T$ < 50 K). Note that all the lattice parameters ($a$, $b$ and $c$) exhibit deviation from the fitting curve below 50 K.

**3.2.2. Atomic positions, interatomic distances and ADPs**. For the data collection at 55 K, a total of 2118 Bragg reflection intensities up to $\sin\theta/\lambda \simeq 1.1$ Å$^{-1}$ [$\lambda$ = 0.552 (1) Å] were measured with the single-crystal neutron diffractometer

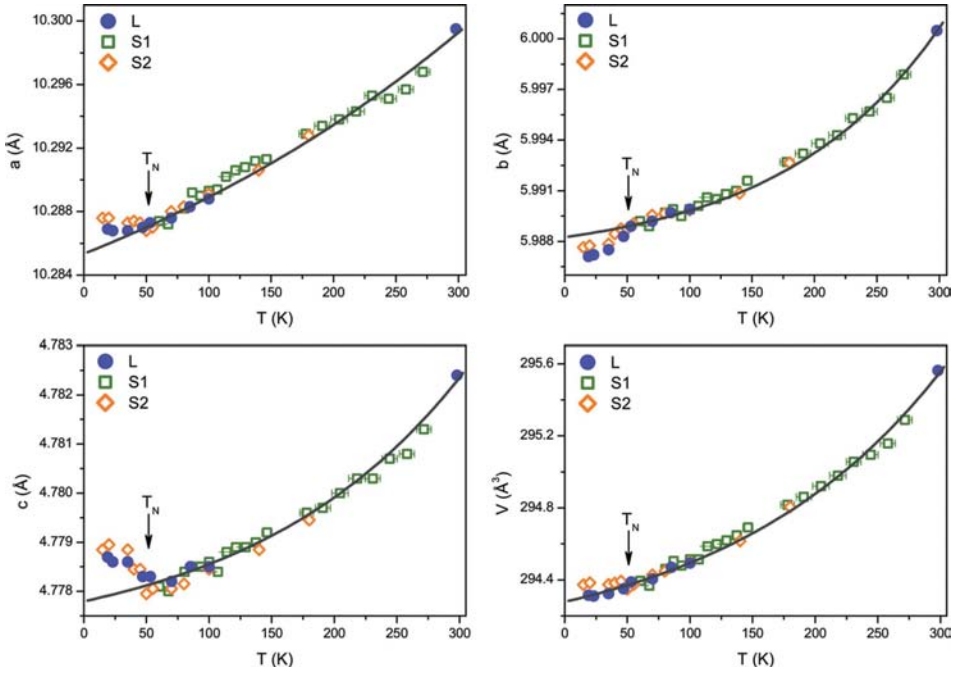


**Figure 6**
Temperature dependence of the lattice parameters and the cell volume of $Co_2SiO_4$. Closed and open symbols represent the results of our laboratory (L) and synchrotron (S1,S2) X-ray diffraction measurements, respectively. In the last case, squares and rhombs mark the results of measurements during the cooling (S1) and heating (S2) procedures, respectively. Error bars from the refinement are smaller than the symbols. The solid curves represent a fit of the lattice parameters in the temperature range from 51 to 300 K (see details in the text).

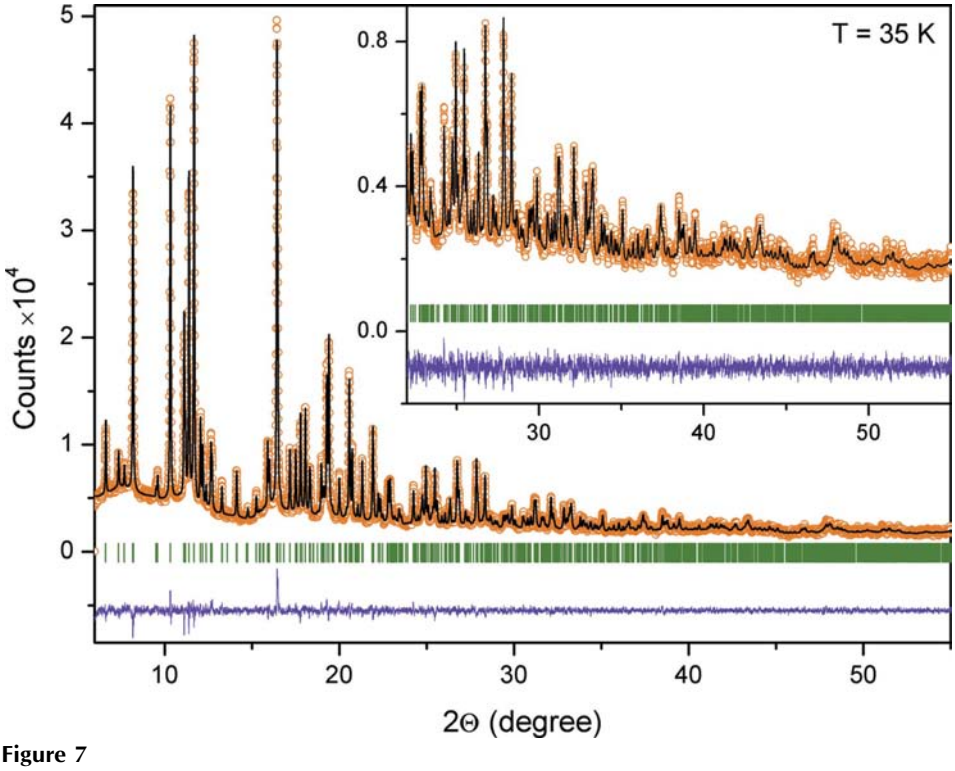


**Figure 7**
High-resolution synchrotron powder diffraction data (open circles), Rietveld fit (line above) and allowed Bragg reflections (tick marks) for $Co_2SiO_4$ at 35 K. The lower trace is the difference, $I_{obs} - I_{calc}$, on the same scale. A magnified view in the $2\theta$ range from 22 to 55° is inserted.

HEiDi. After averaging over all symmetry equivalents, 1465 independent reflections remained ($R_{int}$ = 0.028). A total of 1098 reflections satisfied the criterion $I>2\sigma(I)$ and were used for the structure refinement. A data collection at 2.5 K was also performed up to $\sin\theta/\lambda \simeq 1.1$ Å$^{-1}$ [$\lambda$ = 0.552 (1) Å] and a total of 3226 Bragg reflection intensities were measured. After averaging 1424 independent reflections remained ($R_{int}$ = 0.033). After applying the criterion $I>2\sigma(I)$, 1070 observed reflections were used for the structure refinement. Results of the refinements at 55 and 2.5 K are shown in Fig. 1. The structural parameters of $Co_2SiO_4$ at 55 and 2.5 K are presented in the CIF. The data for the selected interatomic distances and angles in $Co_2SiO_4$ are summarized in Table 3.

Increasing temperature causes a smooth, almost linear increase of the average Co—O distance (Fig. 8). The individual interatomic distances change in the same way as the average one except for the Co2—O2 distance which remains constant within experimental error. In general, variations of the interatomic distances with temperature are small (Table 3) and make up less than 1% in the case of the average Co—O interatomic distance.

In silicate compounds isolated $SiO_4$ tetrahedra generally behave as rigid units if a parameter of state like the temperature is changed. This also holds true for $Co_2SiO_4$. Only minor changes in the $SiO_4$ geometry are observed. The average Si—O distance remains constant within experimental error for the complete temperature range studied (Table 3).

The temperature dependencies of the atomic displacement parameters of $Co_2SiO_4$ are shown in Fig. 9. At very low temperatures, the thermal motion is close to constant at the zero-point motion.

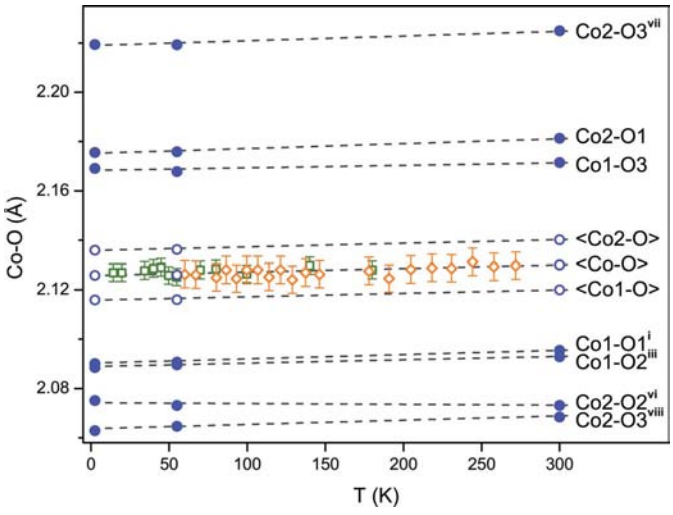


**Figure 8**
Temperature dependence of the Co—O distances for $Co_2SiO_4$. Closed and open symbols represent individual and averaged lengths, respectively. Circles mark the results of our single-crystal neutron diffraction measurements (error bars from the refinement are smaller than the symbols), whereas squares and rhombs mark the results of synchrotron diffraction measurements during the cooling and heating procedures, respectively. The fits are used as guides to the eye. See Table 3 for the symmetry codes.

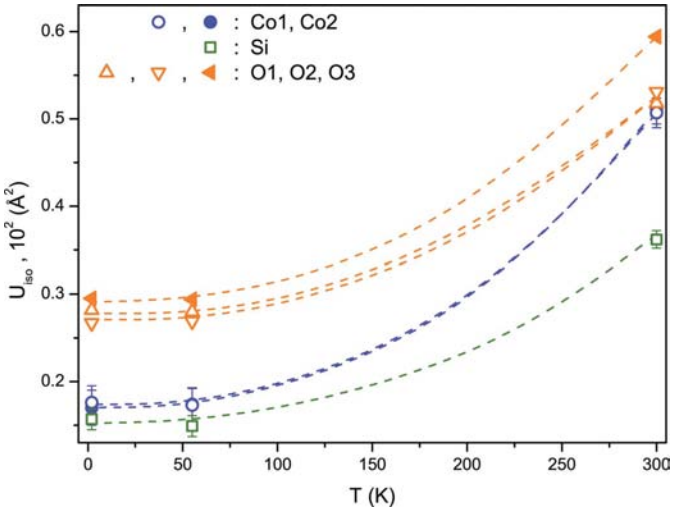


**Figure 9**
Temperature dependence of the isotropic ADPs for $Co_2SiO_4$ according to the results of our single-crystal neutron diffraction measurements. The fits are used as guides to the eye.

The equivalent ADPs of Co1 and Co2 as well as of O1 and O2 are very similar and much larger than that of Si at room temperature. At low temperatures all ADPs remain constant, at least between 55 and 2.5 K. The values for Co1, Co2 and Si are now very similar and almost two times smaller than those of the O atoms.

## 4. Conclusions

Detailed structure analyses on $Co_2SiO_4$ were performed by single-crystal neutron diffraction using a short wavelength of 0.552 (1) Å in the temperature range from 300 down to 2.5 K. Measurements up to $\sin\theta/\lambda < 1.1$ Å$^{-1}$ yielded precise structure parameters for all atoms including O atoms. The data at room temperature are in good agreement with former X-ray results. There is no indication of any structural phase transition below room temperature down to 2.5 K. The interatomic distances and angles as well as the atomic displacement parameters behave quite normally. The lattice parameters of $Co_2SiO_4$ were determined by both laboratory and synchrotron X-ray powder diffraction studies in the temperature range from 15 to 300 K. There is a clear indication of a small but significant anomaly in the anisotropic lattice expansion at the temperature of the magnetic phase transition at 50 K. Below this temperature the lattice parameter *b* is shortened abruptly, whereas *c* increases and *a* keeps constant. However, the resulting volume of the unit cell continues its smooth decrease and does not reflect this anomaly. We assume this anomaly as being caused by magnetostriction.

This work was partially supported by the German Federal Ministry for Education and Science (BMBF projects 03HE6AA3 and 03HE7AAC). The HASYLAB/DESY support at beamline B2 is also acknowledged. One of the authors is grateful to Andreas Berghaeuser for his help with the maintenance of the closed-cycle cryostat.

## References

Ballet, O., Fuess, H., Wacker, K., Untersteller, E., Treutmann, W., Hellner, E. & Hosoya, S. (1989). *J. Phys. Condens. Matter*, **1**, 4955–4970.
Bragg, W. L. & Brown, G. B. (1926). *Z. Kristallogr.* **63**, 538–556.
Brandenburg, K. (1999). *DIAMOND*, Version 2.1c. Crystal Impact GmbH, Bonn, Germany.
Ghose, S. & Wan, C. (1974). *Contrib. Mineral. Petr.* **47**, 131–140.
Ihringer, J. & Küster, A. (1993). *J. Appl. Cryst.* **26**, 135–137.
Knapp, M., Baehtz, C., Ehrenberg, H. & Fuess, H. (2004). *J. Synchrotron Rad.* **11**, 328–334.
Knapp, M., Joco, V., Baehtz, C., Brecht, H. H., Berghaeuser, A., Ehrenberg, H., von Seggern, H. & Fuess, H. (2004). *Nucl. Instrum. Methods A*, **521**, 565–570.
Lottermoser, W. & Fuess, H. (1988). *Phys. Status Solidi A*, **109**, 589–595.
Matsui, Y. & Syono, Y. (1968). *Geochem. J.* **2**, 51–59.
Meven, M., Hutanu, V. & Heger, G. (2007). *Neutron News*, **18**, 19–21.
Miyake, M., Nakamura, H., Kojima, H. & Marumo, F. (1987). *Am. Mineral.* **72**, 594–598.
Morimoto, N., Tokonami, M., Watanabe, M. & Koto, K. (1974). *Am. Mineral.* **59**, 475–485.
Müller-Sommer, M., Hock, R. & Kirfel, A. (1997). *Phys. Chem. Miner.* **24**, 17–23.
Nomura, S., Santoro, R., Fang, J. & Newnham, R. (1964). *J. Phys. Chem. Solids*, **25**, 901–905.
Rodríguez-Carvajal, J. (1993). *Physica B*, **192**, 55–69.
Tamada, O., Fujino, K. & Sasaki, S. (1983). *Acta Cryst.* B**39**, 692-697.